Development of a microfluidic droplet-based microbioreactor for microbial cultivation

Journal:	*ACS Biomaterials Science & Engineering*
Manuscript ID	ab-2019-01668h
Manuscript Type:	Article
Date Submitted by the Author:	03-Nov-2019
Complete List of Authors:	Ho, Chee Meng; Griffith University, Queensland Micro- and Nanotechnology Centre Sun, Qi; University of Queensland, Australian Institute for Bioengineering and Nanotechnology Teo, Adrian; Griffith University, Queensland Micro- and Nanotechnology Centre Wibowo, David; University of Queensland, Griffith Institute for Drug Discovery Gao, Yongsheng; Griffith University, School of Engineering Zhou, Jun; Griffith University Nguyen, Nam-Trung; Griffith University, Queensland Micro- and Nanotechnology Centre Huang, Yanyi; Peking University, Tan, Say Hwa; Griffith University, Queensland Micro- and Nanotechnology Centre Zhao, Chun-Xia; University of Queensland, Australian Institute for Bioengineering and Nanotechnology

Development of a microfluidic droplet-based microbioreactor for microbial cultivation

Chee Meng Benjamin Ho[1#], Qi Sun[2#], Adrian J.T. Teo[1], David Wibowo[3], Yongsheng Gao[4], Jun Zhou[5], Nam-Trung Nguyen[1], Yanyi Huang[6], Say Hwa Tan[1], Chun-Xia Zhao[2*]*

1 Queensland Micro- and Nanotechnology Centre, Griffith University, 170 Kessels Road QLD 4111, Brisbane, Australia

2 Australian Institute for Bioengineering and Nanotechnology, The University of Queensland, St. Lucia, QLD, 4072, Australia

3 Centre for Cell Factories and Biopolymers, Griffith Institute for Drug Discovery, Griffith University, Nathan QLD 4111, Australia

4 School of Engineering, Griffith University, 170 Kessels Road QLD 4111, Brisbane, Australia.

5 School of Information and Communication Technology, Griffith University, 170 Kessels Road QLD 4111, Brisbane, Australia.

6 Department of Advanced Materials and Nanotechnology, College of Engineering, Peking University, 100084 Beijing, China

# These authors have equal contribution.

Corresponding Authors*; E-mail: sayhwa.tan@griffith.edu.au; z.chunxia@uq.edu.au

Abstract

Droplet microfluidics creates new opportunities for microbial engineering. Most microbial cultivation are carried out in bioreactors which are usually bulky and consume large amount of reagents and media. In this paper, we propose a microfluidic droplet-based microbioreactor for microbial cultivation. A microfluidic device was designed and fabricated to produce many droplet-based microbioreactor integrated with an AC electrical field for the manipulation of these microbioreactors. Droplets encapsulating fluorescent *E. coli* cells were generated, sorted and trapped individually in small chambers. Fluorescence intensity was monitored to determine cell growth. An electrical field with varying voltages and frequencies manipulates the droplets, simulating an oscillation effect. Initial results showed that electrical field does not affect cell growth. Comparison with the shake flask showed that a similar standard growth curve is obtained when cultivating at room temperature. This device has the potential for making droplet-based microbioreactors as an alternative for microbial engineering research.

KEYWORDS: Microbioreactor, Microfluidics, *E. coli*, Oscillation and AC electric field

Introduction

Bioreactors are important tools for cell culture and fermentation in which researchers can gain better insights into the functions of microorganisms at molecular and genetic levels [1]. The ability to effectively control various bioprocess conditions in bioreactors, such as temperature, pH, agitation, and dissolved oxygen (DO) levels [2-4] results in valuable physiological and metabolic information at different stages of the fermentation process [1]. Although conventional automated stirred-tank bioreactors provide extensive control over the cell culture environment, reliability, and generation of information-rich data, they are typically too expensive and labour-intensive for screening purposes. Bench-scale bioreactors, despite its improvement in recent years with the reduction of reactor volume and increment of the number of parallel operating reactors [5], remain expensive due to the sophisticated measurement devices inherent in the bioreactors and the time-consuming efforts for sterilisation and sensor calibration. Simple bioreactors, i.e., test tubes, shake flasks, and microplates, are nonetheless still widely used in laboratories [6-8]. The main advantages of microplates (typically containing 24 or 96 parallel wells) are their small working volumes (typically ranging from 0.1 to 3 mL per well [9-10]), high throughput, and automated experimental set-up. However, the microplates have limited control over the bioprocess conditions, and the data obtained are often limited to endpoint measurements. Therefore, there is currently a gap for further development of microplates as high throughput microreactor systems with extended measurement points and parameter controls [1].

The thought of microbioreactors with integrated sensors combining the small volumes of microplates with the monitoring and control features found in bench-scale systems forms the idea of a promising tool for rapid, high throughput, and cost-effective screening [1]. If a bioreactor could be miniaturised into the micrometer scales, it would bring about numerous new applications, such as biosensors, microfermentor arrays, or microbiological assay kit. A possible technology in making that happen would be using microfluidics. While most microfluidic research efforts to date have concentrated on eukaryotic cell biology [11-12], microfluidics is slowly making its impact on microbiology [13-14]. Its scale of size matches well with the physical dimensions of most microorganisms, and micron-scale tools enable various manipulation on individual cells, their immediate extracellular environments (referred to as the microenvironment), shape and internal

organisations [13, 15]. Most microfluidic devices are fabricated using soft lithography with poly(dimethylsiloxane) (PDMS). Soft lithography provides a fast and versatile fabrication technique, while PDMS provides attractive materials properties such as biocompatibility, transparent, and flexibility [16-17]. Microfluidics is expected to play several significant roles in advancing microbiology by precisely controlling local microenvironments surrounding microbial cells, by isolating and studying individual or small groups of cells, and by providing identical and reproducible culture conditions and therefore generating quantitative data [1, 6]. This is further shown with microbial microbioreactors where applications focus on screening strains and examining growth parameters [18-25].

An integrated microfluidic microbioreactor (μbr) indeed have clear advantages like small volume, single-use, and high throughput. However, it is important to bear in mind that most reactors consist of one reaction and require extensive handling of tubing when the scale increases. Recently, droplet microfluidics has become one of the key technologies that is opening up new experimental possibilities in biology [6]. It offers numerous advantages by encapsulating cells in individual droplets [26]. Firstly, a single cell can be isolated into its own tiny liquid compartment. These stochastic confinements allow biochemical products secreted by cells to accumulate faster as compared to cells that live in a bulk culture, thereby reducing biochemical production times. Secondly, the ability to upscale from few to thousands of droplets allows droplet microfluidics to be a high throughput analysing tool that is versatile and powerful. Finally, it offers precision control of the local environment, enabling researchers to study topics relating to growth, mobility, adhesion, and chemical communication of cells, as well as the collective behaviour and response of a cell population, which in turn offers a brand-new scientific knowledge [27-28].

In this paper, we developed a droplet-based microfluidic microbioreactor for microbial cultivation. For this μbr, we used a T-junction for generating uniform monodisperse droplets that encapsulated a small number of bacteria. The design contained individual traps that allowed for capturing of sorted droplets while preventing the coalescence from the following droplet. Once a suitable device had been fabricated, microorganism compatibility and device performance were evaluated using engineered *Escherichia coli* (*E. coli*) producing green fluorescent proteins (GFP). Droplet size and bacteria viability images and videos were all captured using a fluorescence camera and

analysed using a customised written program by MATLAB. For manipulating the droplets, an electrical field with square wave modulation was applied, giving an oscillation effect on the *E. coli*. Our initial results showed that *E. coli* could grow normally in both static and oscillating droplets. A stable growth of *E. coli* was also achieved with the use of our droplet-based microfluidic μbr device as compared to the use of a shake flask. This shows that our microfluidic device is stable and possesses the possibility of upscaling for further applications. The development and utilisation of this device for culturing and investing the growth or studies of microorganisms represent the first step in realising a fully integrated device towards high throughput microorganism fermentation.

Materials and methods

Fabrication of the microbioreactor device

The microfluidic devices were fabricated using standard photo-lithography and soft-lithography techniques [29-30] with SU-8 (Microchem SU-8 3050) and PDMS (Sylgard 184, Dow Corning, USA) respectively. Briefly, SU-8 was spin-coated (Laurell WS-650-23 B) at 1100 rpm for 30 s and dried at 95^{o}C for 40 mins. This baked wafer was then exposed to UV-light for 5 s with the patterned mask and baked at 95^{o}C for 7 mins. Unpolymerised regions of the SU-8 were removed by soaking and spraying the wafer with the SU-8 developer. This protocol gives us approximately 100 μm in depth. Replicas of this mold were patterned by using PDMS in the standard 10:1 ratio (silicone elastomer base: curing agent) and heated to 80^{o}C for at least 1 h. The inlets and outlets of the PDMS device were punched and washed with isopropanol before being irreversibly bonded to a glass chip with an oxygen plasma activation. Electrodes were made using indium alloy (Indium Corporation, USA) for the generation of an AC electric field. Chips were surface-treated with Aquapel (PPG Industries, USA) through the inlets, and the residues after the surface treatment were flushed out with pressurised air.

Bacterial strain, growth media and cultivation conditions

E. coli producing green fluorescent protein (GFP) (ATCC® 25922GFP™) was purchased from the American Type Culture Collection (ATCC, Manassas, VA). This strain was selected in this study due to the relative ease of recombinantly producing GFP and the ability to easily quantify fluorescence intensities in cell cultures. To cultivate the *E. coli*, a single colony selected from a

freshly streaked Luria-Bertani (LB) agar plate (10 g/L tryptone (BD Biosciences, Australia), 5 g/L yeast extract (Merck, Australia), 10 g/L NaCl (Chem-Supply, Australia), 5 g/L agar (Amresco, USA)) was inoculated into 5 mL LB media (10 g/L tryptone, 5 g/L yeast extract, 10 g/L NaCl) and incubated at 30°C with a shaking of 150 rpm overnight. The overnight cell culture (1 mL) was seeded into a 50-mL falcon tube containing 10 mL of fresh LB media and then incubated at 37°C, 150 rpm until an optical density at 600 nm (OD_{600}) reached approximately 0.6 before loading the cell culture into the microfluidic device. All media for bacterial cultures were sterilised by autoclaving at 121°C for 15 mins and, after cooled them down, supplemented with 100 µg/mL ampicillin (Gibco, USA).

Microfluidic set-up

Before the start of each experiment, a new fully function microfluidic device was mounted onto an inverted microscope (Nikon Ti-E, Japan) that was equipped with two cameras to capture the video (Phantom Miro 3,Vision Research Inc) and the fluorescence images (TrueChrome Metrics, Tucsen). A heating glass (HG-S-Z001, Live Cell Instrument) was adapted on the microscope stage for controlling and maintaining a constant temperature throughout the experiments. Two temperatures settings 27°C and 40°C were used in this set-up which maintained the device temperature at 25°C and 37°C, respectively. PTFE tubings were connected to the inlets of the device with the other end connected to the glass syringe. Three glass syringes were used; one channel is for the dispersed phase *E. coli* GFP suspensions and the other two channels are for the continuous phase mineral oils (Cat. No. M5904, Sigma-Aldrich, Australia) with 2 wt% of Span® 80 (Cat. No. S6760, Sigma-Aldrich, Australia). The glass syringes were all controlled with syringe pumps with adjustable flow rates (NEMESYS). For generating an electrical field, the device was connected onto an alternating current electric generator (33210A, Agilent) and amplifier for electrical modulation. Each experiment was repeated three times with images of five control droplets and five experimental droplets taken at 30-min intervals. Two types of images, i.e., fluorescent and white lights, were captured. The images were then processed using a customized MATLAB programmed to determine the fluorescence intensities.

Image analyses

Images and videos obtained from all experiments were recorded and analyzed using MATLAB. To measure the fluorescence intensity, a binary mask was needed for extracting the location and size of the droplet, which can be operated both automatically or manually. For the automated process, droplet images from the white light images were detected as circles using Circular Hough Transform (CHT) algorithm which is robust to noise, occlusion and varying illumination. Once the droplet was detected, CHT algorithm may return multiple results (circles) for each droplet. An interactive process was developed so that the user can select the best circle from top ten candidates provided. The circle chosen was then given as a binary mask. If the circle could not be detected, image segmentation technique would be used to trace the outline of the droplet before converting it to a binary mask. The fluorescence videos or images corresponding to their own binary mask were then analysed. The data files were first converted from colour images into grayscale images. The mean values of the grayscale images were calculated based on the area covered by the binary mask generated earlier. The output indicated the fluorescence intensity. For the video files, the program processed through each frame and calculated its intensity. It is important to note that the binary mask must be applied to each droplet individually while the calculation steps can run automatically. The code will be shared upon request.

Results and discussion

Design of droplet-based microfluidic µbr device

In this study, a droplet-based microfluidic µbr device was designed to form water droplets encapsulating bacteria cells and developed it as a bioreactor for the microbial cultivation. Recombinant *E. coli* producing green fluorescent protein (*E. coli* GFP) were used as a model bacterium. To cultivate *E. coli* GFP, the µbr device was designed to consist of four key components: (1) droplet generation, (2) droplet sorting, (3) droplet trapping and (4) droplet oscillation (**Figure 1**). In the droplet generation, a T-junction was used to mix a continuous oil phase (mineral oils containing 2% of Span® 80) and a dispersed water phase (*E. coli* GFP in an LB medium), thus, forming water-in-oil emulsion droplets encapsulating *E. coli* GFP (**Figure 1**, blue box). To sort droplets of uniform size, an additional fluidic inlet (secondary mineral oil) was introduced at a controlled flow rate to assist in sorting the droplets and direct them to the upper channel (**Figure 1**, red box). The sorted droplets were flowed further entering the droplet trapping region which contained a total of 40 traps nearby the electrodes. The 10 traps were located before the electrodes,

20 traps in between the electrodes, and 10 traps after the electrodes, aiming to provide a better reading (**Figure 1**, purple box). Additionally, in this droplet trapping region, an exhaust channel built at the back of the trap allowed the continuous oil phase to flow through when the trap was empty. Once a droplet was trapped, the exhaust channel caused the emulsion flow to terminate and another droplet to enter [31]. The droplets trapped in between the electrodes were exposed to an AC electric field of various frequencies and amplitudes deforming the droplets at a constant speed and creating oscillation effects (**Figure 1**, purple box).

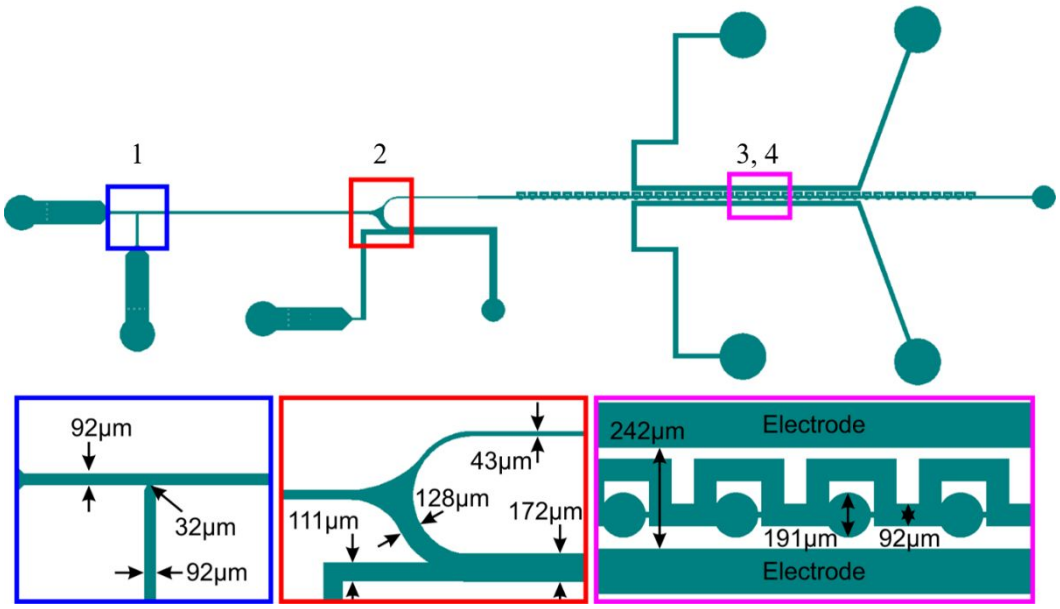

Figure 1. Schematic diagram of the microchip design and its critical dimensions. (1) Blue boxes: The T-junction for a water-in-oil droplet formation with the dimension shown for the continuous fluid channel and the dispersed fluid orifice. (2) Red boxes: The structure of droplet sorting with the curved path dimensions. (3, 4) Purple boxes: The structures of both droplet trapping and droplet oscillation regions along with the dimensions of continuous fluid channel, traps, and a gap between both electrodes.

To generate water-in-oil droplets in the microfluidic T-junction, the flow rates of the continuous phase (**Figure 2**a, orange) and the dispersed phase (**Figure 2**a, blue) were controlled at 150 and 30 μL/min, respectively. At this stage, the droplet size can be varied by controlling the initial flow rates of water and/or oil phase (**Figure 2**b). Prior to entering the droplet sorting region, the droplets from the droplet generation region would be decelerated due to the increase in the channel size and exited through the lower channel following the default streamline in which it was positioned.

A secondary oil phase was then introduced for sorting the droplets achieving a uniform size of droplets as well as for directing the droplets into the designated chambers using hydrodynamic actuations. By controlling flow rates of the secondary oil between 1000 and 6500 µL/min, the flow rate of droplets could be slowed down, and the flow streamline could be changed to the opposite direction, thus causing droplets from different directions to collide to each other and to force some droplets moving into the upper channel (**Figure 2**c). Further increasing the flow rate of the secondary oil to higher than 6500 µL/min caused all the droplets to flow into the upper channel and eventually followed by droplet coalescence, hence, diminishing the droplet sorting capability (Supplementary Figure S.1). In the upper channel, the droplets were trapped individually into individual chambers before the flow rates of the fluids were reduced to 10 µL/min (**Figure 2**d). In this way, the trapped droplets could be prevented from flowing back into the sorting chamber. The trapped individual droplets encapsulated with bacteria were then exposed to AC electric field using a 50 kHz sine wave with varying electrical amplitude (100 to 400 Vrms) and square modulation frequency (1 to 100 Hz) providing a dynamic environment for cells to grow (**Figure 2**e).

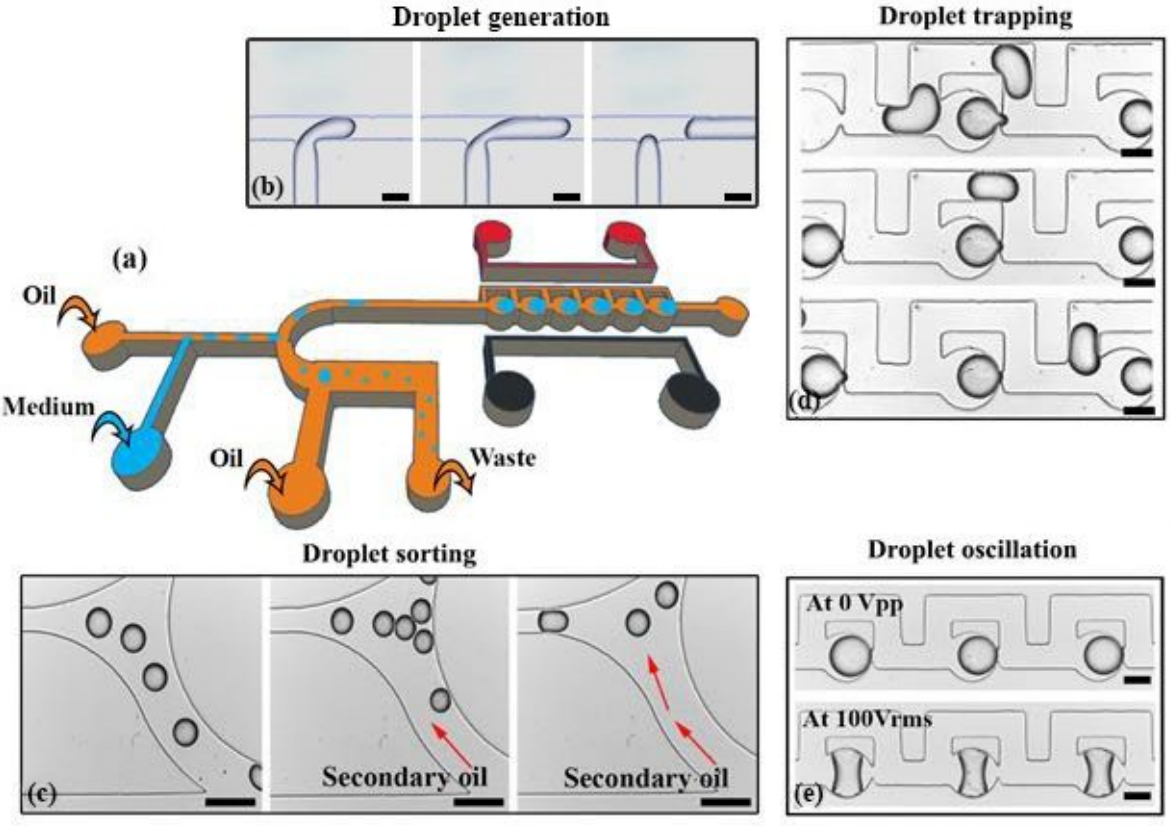

Figure 2. Design of the microfluidic microbioreactor (µbr) for droplet formation, sorting, trapping and oscillation. (a) Schematic illustration of the droplet-based microfluidic platform. The platform

consists of four main components: (b) Droplet generation; (c) Droplet sorting: flowing the secondary oil at a controlled flow rate sorted the droplets to a uniform size and simultaneously changed the droplet flow direction toward the upper channel as indicated by the red arrows; (d) Droplet trapping; and (e) Droplet oscillation under the AC electrical field at 100 Vrms which caused the trapped droplets to deform. Scale bar = 100 μm.

Characterisation of μBr

As droplets act as a microreactor for *E. coli* cultivation, it is important to maintain the reaction volume or to characterise any volume variation. An initial droplet stability test was performed by using droplets of approximately 120 μm in diameter which were deposited in the integrated trap structures and incubated at 37°C for a period of 100 mins at 37°C (**Figure 3**A). Images of droplets were taken at 10-min interval, and droplet volume percentages were measured and calculated using our customised MATLAB program and ImageJ for verification (procedures can be found in S2). The results clearly showed that droplet size was slowly decreasing over 100 mins with a 50% decrease in droplet size at 90-min (**Figure 3**A, a–h). Droplet size plays an important part in fluorescence experiment as we want to ensure that the fluorescence intensity is due to the increase in cell growth rather than the accumulation of GFP protein when the droplet shrink. Droplet shrinkage occurrence is mainly due to the porosity of the PDMS matrix, the shearing by continuous phase flow rate [31-33], and the evaporation (as the device temperature was maintained at 37°C to provide an optimal growth condition for *E. coli*). To assess cell viability and protein expression within the droplet, *E. coli* containing a multicopy vector encoding the green fluorescent protein (GFP) mut3 was used. Due to the mutation in the GFP, its fluorescence intensity can be detected within 8 min after induction of the *E. coli* growing in the log phase, as compared to wild type GFP which is detectable after 1 to 2 h of growing *E. coli* under identical conditions[34]. This coupled with doubling time of the *E. coli* of approximately 15 to 20 min allowed us to monitor the fluorescence intensity at least for two cell cycles. Droplets were imaged at every 10-min interval and the fluorescence intensity was measured. **Figure 3B** shows fluorescence intensity increasing after 20 mins, indicating that the bacteria were able to proliferate, and the shrinkage of droplets did not affect their growth after 40 mins. It was previously shown that fluorescent protein did not leak out of the continuous phase thus allowing us to continue monitoring the bacteria within the droplet [31]. Based on this result, for observation of *E. coli* growth, the flow rate of the continuous phase was

increased from 30 µL/min to 40 µL/min which also caused the droplet size to increase from 150µm to approximately 180 µm, respectively. While lowering the temperature to 25°C caused the rate of droplet shrinkage to slow down, this gave us enough time (~3 h) to properly observe at least a few growth cycles of *E. coli* to obtain a substantial result.

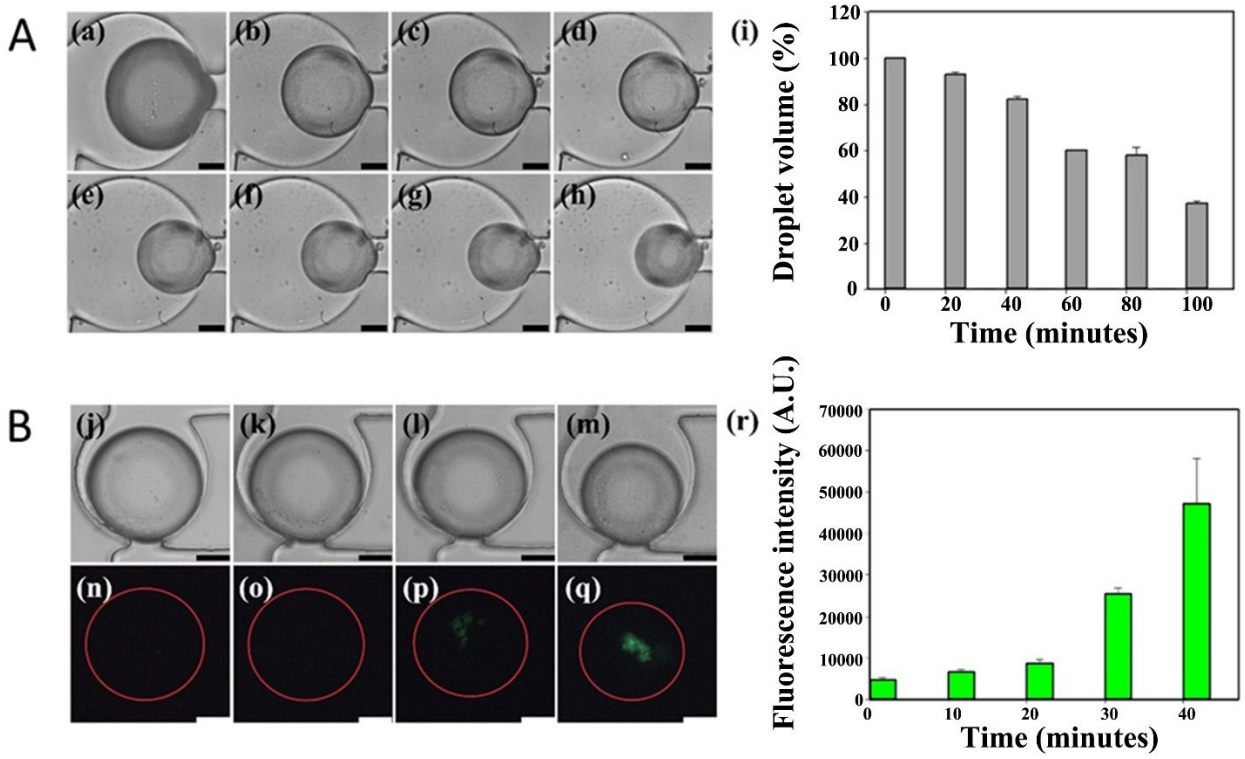

Figure 3. Droplet stability over time at 37°C and bacteria viability testing. A) A decrease in droplet volume was observed over a period of 100 mins. (a) to (h) show images of droplet size while (i) shows the volume percentage decrease over a period of 100 mins. B) Fluorescence intensity over time for 40 mins. (j) to (m) White light images droplets and (n) to (q) fluorescence imaging of encapsulated bacteria respectively. Scale bar represent = 50μm

To observe and analyse *E. coli* growth in the immobilised droplets, the intensity of GFP generated was quantified using the epifluorescence microscopy. Droplets were constantly observed with a fluorescence camera. The evaluation processes of images and videos were automated to aid us in speeding up the processes. As a result, settings for the images were maintained constant and characterised before any experiment. Important factors such as the camera settings as well as the microscope settings were taken into consideration. The camera settings were determined by using the default setting of the camera initially (as the control). Normal and fluorescence images of

encapsulated bacteria droplet were taken before changing the camera settings one at a time while capturing new images. Different camera settings were then compared against the control. The camera was manually set, and the automatic function was not used to determine the optimal setting. Our results showed that exposure (the amount time the light is exposed to the cells), gain (light sensitivity of the camera), contrast (difference in color and brightness), and gamma (value of pixel relates to actual brightness) played a significant part in affecting our images for different experiments (**Figure 4**a), whereas other camera settings, including saturation and sharpness, did not (Supplementary Figure S3). Furthermore, as the fluorescent bacteria were freely moving in the droplet, images of the droplet at different z-planes (set as the microscope setting) were captured for observing whether this movement might affect the readings. However, adjusting the z-plane capture did not have any significant difference (Supplementary Figure S3) and this allowed us to capture the bacteria on a fixed plane. One major issue with the use of fluorescence protein is photobleaching. It is the process by which repeated cycling of the fluorophore between ground and excited states eventually lead to molecular damage with a gradual reduction of fluorescence emission intensity from a sample over time [35]. As droplet with fluorescence *E. coli* will be constantly exposed to the UV light, it was important to ensure what was recorded is as accurate as it can be. By adjusting the transmission intensity of the lamp (Nikon, C-HGFI HG Fiber Illuminator "Intensilight" MBF72655), different droplets with fluorescence *E. coli* were constantly exposed to the light for 30 mins over a 1.5 h period under the two settings, i.e., ND32 (1/32 transmittance power) and ND1 (full transmittance power). The degradation of the fluorophore occurred quickly for ND1 (within 10 mins) as compared to ND32 degradation which was a lot slower (**Figure 4**b). Although photobleaching occurred, by using a lower transmittance, degradation was slowed down which allowed for a longer measuring time to track the growth of *E. coli*. By fixing the camera setting and using a low UV power, it allowed us to obtain for a longer *E. coli* growth with more accurate results.

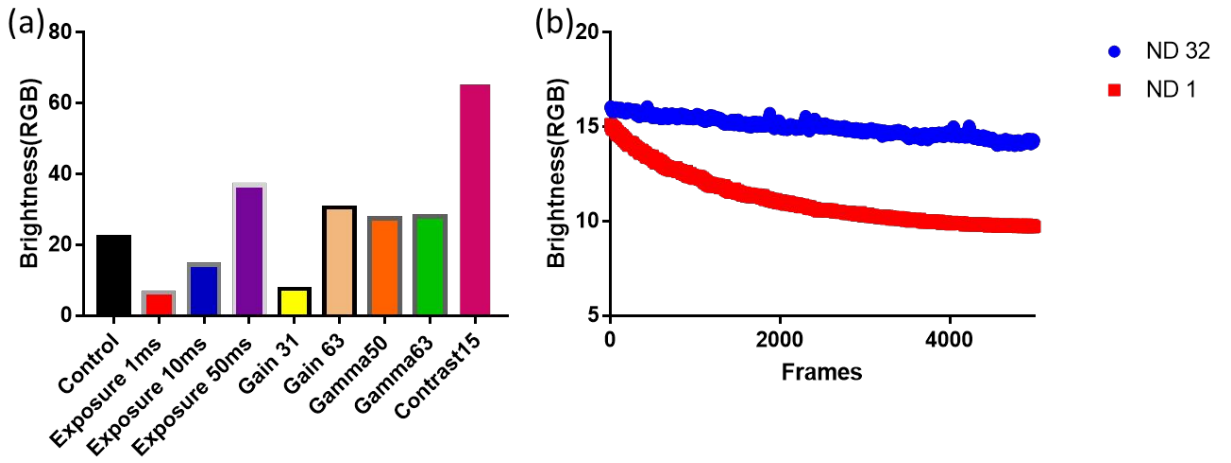

Figure 4. Characterisation of the camera and fluorescence settings that may affect overall results for the system. (a) Camera settings (exposure, gain, gamma, and contrast) and (b) Fluorescence lamp transmittance power (ND32 and ND 1) for 1.5 h of exposure.

Effect of electrical fields

To determine how different voltages may affect growth, the encapsulated *E. coli* droplets that were trapped between the electrodes were exposed to final output sinusoidal voltage of 100, 200, and 400 Vrms. It was previously shown that an AC electric field can induce droplet deformation [30]. Therefore, we decided to use a sinusoidal voltage at a frequency of 50 kHz, as the droplet-shape stability at low frequencies of 20 kHz and below were unstable and the droplet deformation was independent of frequency above 60 kHz. It was also shown that deformation of droplets became stronger with increasing electrical field intensity. In our case, droplets were exposed to increasing intensity of final output (100, 200 and 400 Vrms) which also showed an increase in deformation (the diameter of droplet becoming smaller) (**Figure 5**a). However, voltages higher than 400 Vrms gave similar deformation (approximately 116 µm), thus 400 Vrms was fixed as the upper limit. Droplets were exposed to the electrical field for 30 mins and a 1 min recording of the fluorescent droplet was done. Previous studies have shown that electrostimulation of bacteria reduced proliferation efficiency at higher electrical AC field (5 V/cm at 10 MHz) [36-37]. However, electrical currents were known to induce changes in DNA synthesis, protein synthesis and membrane permeability [38]. To minimise bacterial cell damages due to electrical currents, the electrodes were isolated from the fluidic channel (**Figure 1**), providing insulation against an electrical current, and we used oil as the continuous phase which is a poor conductor of electricity. It was observed that

there was an increase in fluorescence intensity for all the three settings over 3 h (**Figure 5**b). This showed that no damage was occurred to the cells when exposed to an electric field, indicating that bacteria were growing in the droplet with or without an electrical field. Although there was no significant difference between the control and experimental growth rate, bacteria exposed to various voltages appeared to grow slightly faster. Beside comparing between the control and experimental groups, the relationship between voltage parameters and fluorescence was also analysed by an R^2 plot (Supplementary Figure S4). However, overall slope gradient for each timepoint is similar and not significantly different. With increasing voltages, droplets became narrower (**Figure 5**A), possibly allowing better mixing of bacterial cells and nutrients [30], thus improving the bacterial growth. The electrokinetic effects from the electrical field can also play a part in concentrating bacteria within the droplet [39-41]. Most droplets followed the same trend (gradually decreasing approximately 25% over time) except for droplets exposed to 50 kHz, 400 Vrms where there seemed to be a greater drop in size (**Figure 5**C). A possibility could be the turning off and on of the generator for recording the results at every 30-min interval might have caused the "stretching" of droplets and, in doing so, the droplets lose media in the process. Our initial results showed that prolonged exposure to an AC electrical field does not affect the growth rate of *E. coli*, but higher voltages may reduce the droplet size faster. Next, we determined how oscillation of the droplet might improve the growth rate by applying a square wave modulation of 1 Hz.

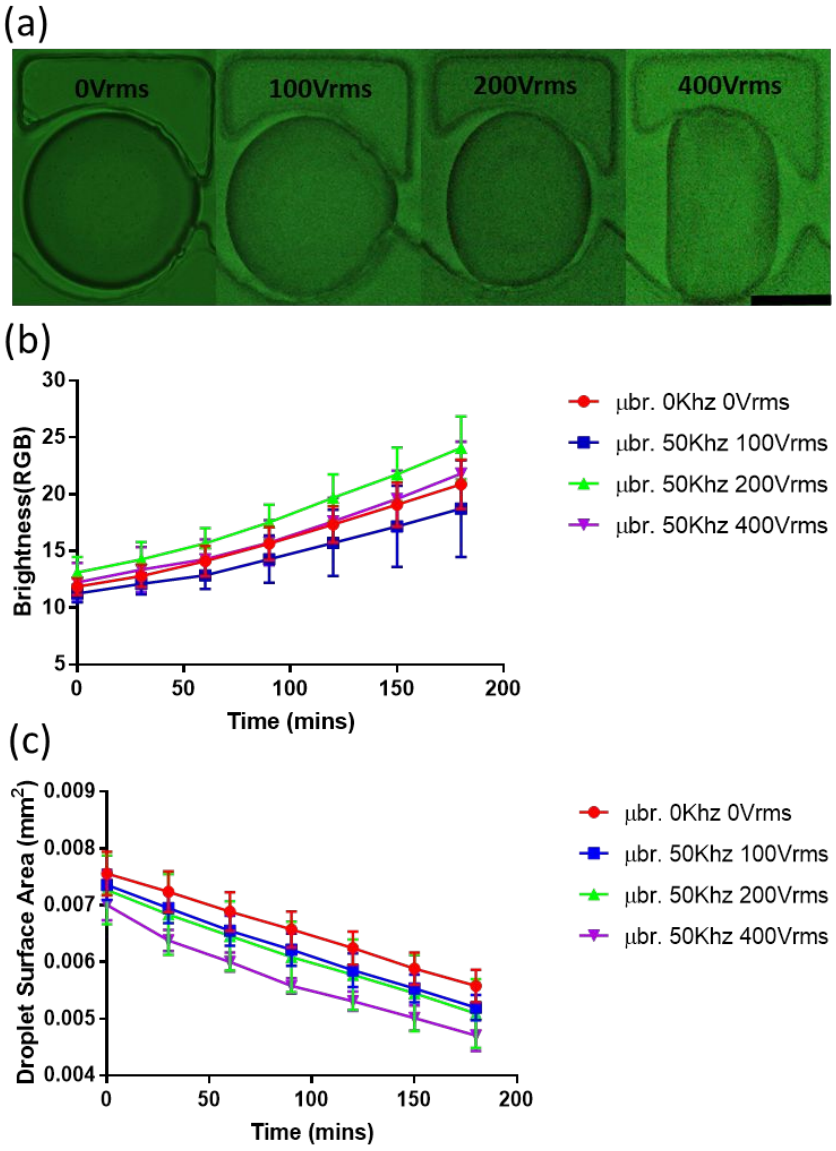

Figure 5. Effects of various electrical fields (EF) applied on the droplets encapsulating *E. coli*. (A) Droplets deformation with various voltages. Scale bar = 100 μm. (B) EF effect of *E. coli* growth. Performing a T-test analysis with control show no significant difference between increasing voltage with the control (n=3) (C) Droplet size over a 3 h period at 25°C for various voltages.

Effect of oscillation

It was shown that the rate of growth and final cell number of *E. coli* increased when liquid culture media is shaken [2, 42]. In bulk culture assays, liquid media must be aerated to provide dissolved oxygen and proper mixing of media. The commonly used way is by vigorous stirring or shaking

the culture flask. One important factor to consider is the surface area of the liquid. By vigorous agitating the liquid media, these mixing techniques provide better mixing and minimize areas of high or low nutrient concentration. To provide a shaking effect for our μBR, droplets manipulation was done by applying a square wave modulation of different frequencies which enable us to create an oscillation effect possibly mixing cells and nutrients. The use of an electrical field allowed for precise control on multiple droplets, causing them to deform and return to its original shape quickly. By using droplets, we hypothesised that with bigger droplet deformation and faster speeds, better agitation may occur leading to a faster growth rate. For simulating faster speeds, oscillation rate was increased by changing frequency of the square wave modulation magnitude from 10 to 100 Hz to oscillate the droplet faster (Supplementary Figure S5). Results indicated that there was no change in the growth rate with increasing frequencies (**Figure 6**). It is possible that at 1 Hz and 10 Hz the speed might not be fast enough, while at 100 Hz the response time of the droplet deformation might be too fast for any deformation to take place. Another possible reason is that the droplet may not contain enough nutrients for the cell to grow quickly. Droplet size decreases gradually with increasing modulation, unlike the deformation in the previous experiment(Figure 5). To summarise, our microfluidics microbioreactor provides an environment that allows upscaling and quick visualisation of *E. coli* cell growth. Initial results showed that electrical field did not affect growth while providing an additional option for manipulating droplets.

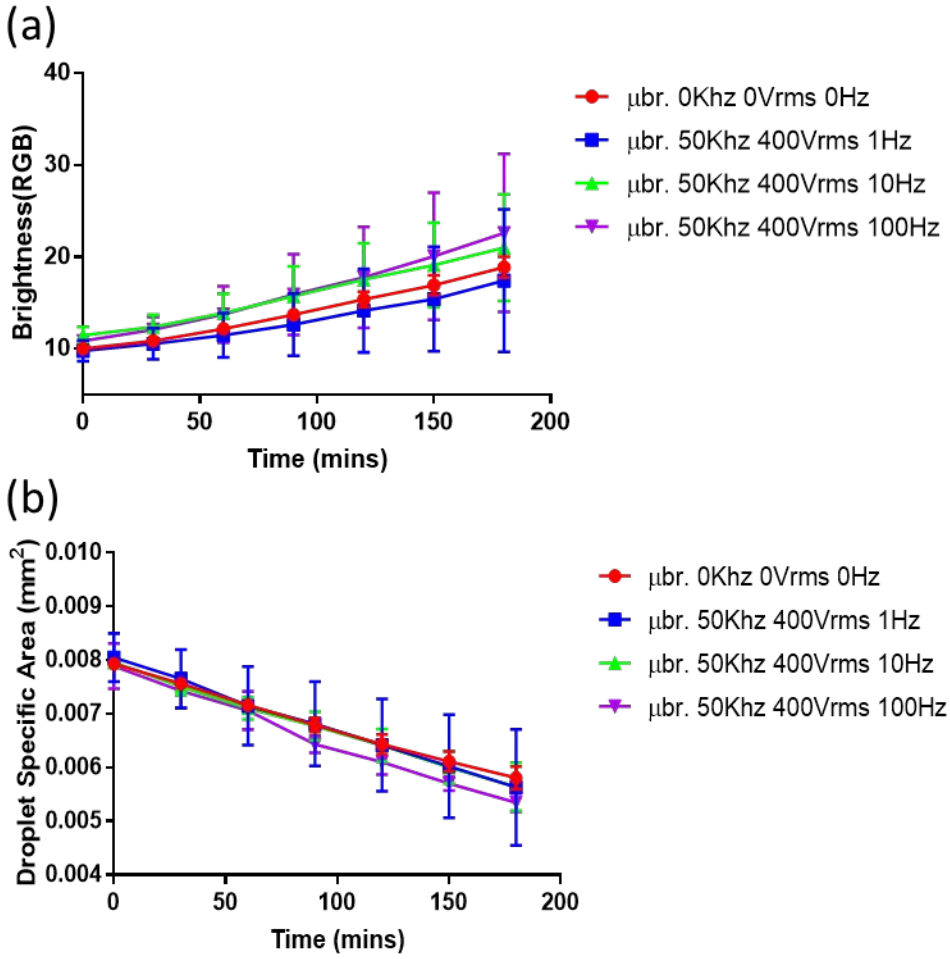

Figure 6. Effects of Oscillation on *E. coli* Growth. (a) Increase oscillation over a 3 h period. (b) Decrease in droplet size over 3 h at 25°C for various frequencies.

Comparison of *E. coli* growth in µbr and in shake flasks

Although, our initial results showed that increasing oscillation did not significantly affect the encapsulated bacteria growth when compared to the control. The next step was to determine the duration in which the microorganism can grow in the droplet and does other growth stages appear during that time. The reason being, cells that are growing healthy initially will slow down when coming into contact with a new environment, therefore a lag phase is produced [43]. For a comparative study, *E. coli* was first grown in a shaker flask at 25 °C and 37°C, with 37°C being the optimal temperature for *E. coli* growth. Cells were measured at 1 h intervals to get their optical density. **Figure 7**a shows cells grown at 37°C were able to reach the stationary phase after 4 h

while cells grown at room temperature were slowly entering the log phase. From the oscillation experiments (**Figure 4**), we noticed that there was a slight increase in growth for 50 kHz 400 Vrms 10 Hz and decided to run with this setting for a longer period. To prevent the droplets from shrinking to quickly, droplets were incubated at room temperature only. Droplet size was found to decrease (approximately 60%) after the 6 h period (Supplementary Figure S6). From this result (**Figure 7**b), it seemed that oscillating droplets for a longer period (6 h) did not have any significant effect on the bacteria growth. Interestingly, we were able to obtain a standard growth curve similar to that of shaker flask grown at 37^{o}C flask rather than that grown at room temperature. As mentioned previously, one major advantage of using droplets as a microbioreactor is its stochastic confinement [6]. This confinement allows for microorganisms or own metabolites [44-45] to accumulate faster resulting in our case a faster growth of *E. coli* (**Figure 7**c). However, it is important to note that further experimentation needs to be done to confirm that cell behavior is similar to the shaker flask at the gene expression level due to the different temperature used.

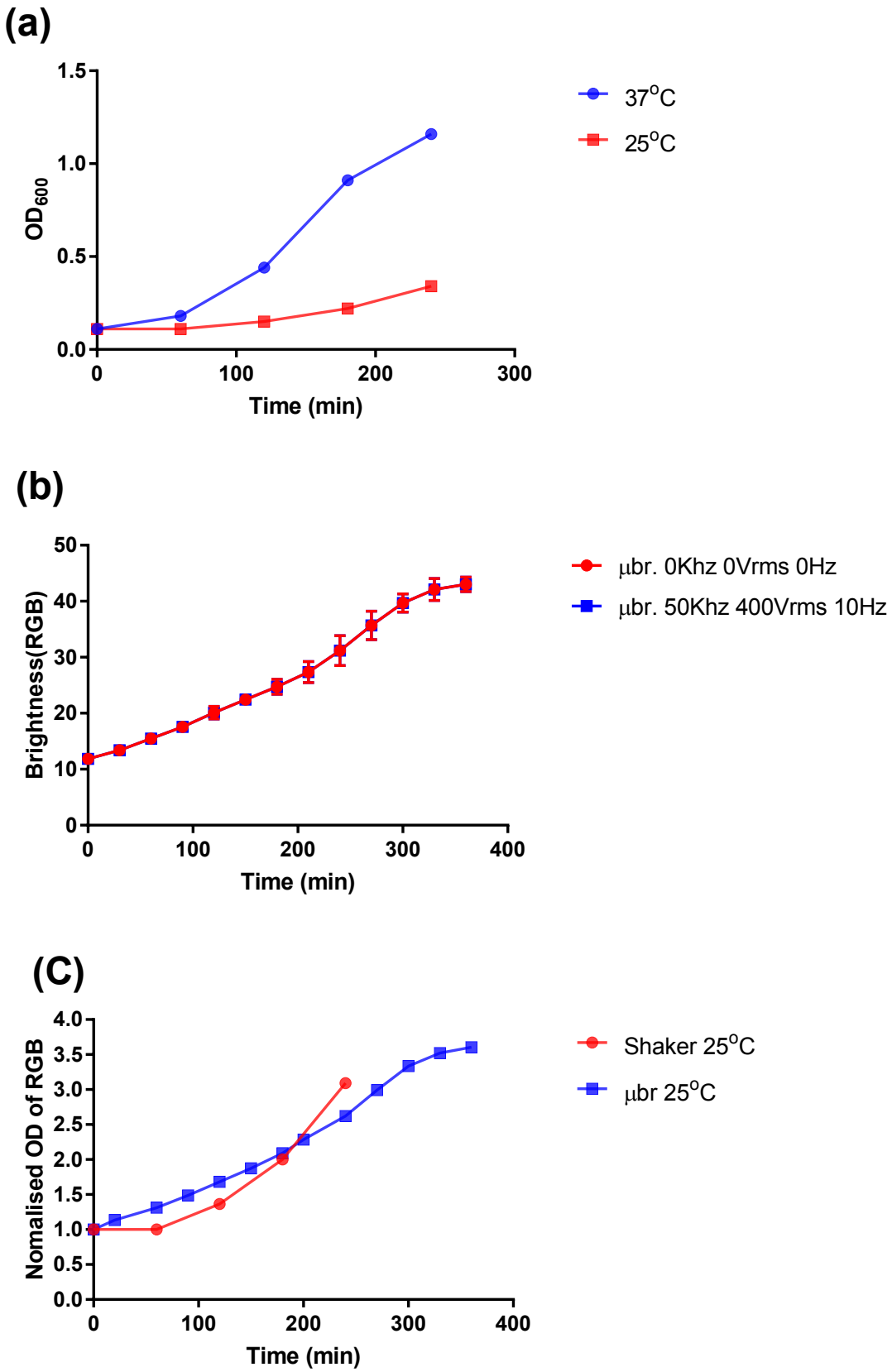
(a)
OD600
1.5
1.0
0.5
0.0
0
100
200
300
Time (min)
37°C
25°C
(b)
Brightness(RGB)
50
40
30
20
10
0
0
100
200
300
400
Time (min)
µbr. 0Khz 0Vrms 0Hz
µbr. 50Khz 400Vrms 10Hz
(C)
Nomalised OD of RGB
4.0
3.5
3.0
2.5
2.0
1.5
1.0
0.5
0.0
0
100
200
300
400
Time (min)
Shaker 25°C
µbr 25°C

Figure 7. Comparisons of the growth of *E. coli* in shake flasks and in droplet microfluidic device μbr.

Conclusions

Droplet microfluidics provides numerous advantages for studying single or small amount microorganism in their own tiny liquid compartment. In this paper, we demonstrated for the first time an AC electrical field induced droplet oscillation μBr for microorganism cultivation. We have shown the possibility of a microfluidic platform generating, sorting and trapping cell encapsulated droplets. By varying the electrical field voltage and frequency, we were able to manipulate droplets, creating an oscillation (shaking effect) of *E. coli*. It was also observed that an AC electrical field did not affect *E. coli* growth, enabling further work with our design. A comparison between a shaker flask and our droplet microfluidic device, showed that encapsulated droplets grown at room temperature were able to obtain a standard growth curve similar to that done in a shaker flask at 37^{o}C within 6 h, a much faster rate than the shaker flask grown at room temperature. This microfluidic device can provide researchers with another solution which is high throughput, cost-efficient and provides a variable environment for cell analysis. However, more experiments must be carried out with different cells types to determine their individual optimal conditions for ideal results. We foresee that this device has the potential for making droplet microfluidics a better alternative for research as it provides a dynamic environment for biological studies.

Acknowledgement

C.X.Z acknowledges financial support from Australian Research Council through the award of an ARC Future Fellowship (FT140100726). S.H.T acknowledges the support of the Australian Research Council (ARC) Discovery Early Career Researcher Award (DECRA) (DE170100600). This work was performed in part at the Queensland node of the Australian National Fabrication Facility funded under the Australian Government's NCRIS program.

References

1. Hegab, H. M.; Elmekawy, A.; Stakenborg, T., Review of microfluidic microbioreactor technology for high-throughput submerged microbiological cultivation. *Biomicrofluidics* **2013,** *7* (2), 021502. DOI: 10.1063/1.4799966.

2. Bates, M. K.; Phillips, D. S.; O'Bryan, J., Shaker agitation rate and orbit affect growth of cultured bacteria. *Thermo Fisher Scientific ANSHORBGRT* **2016,** *816*.
3. Betts, J.; Warr, S.; Finka, G.; Uden, M.; Town, M.; Janda, J.; Baganz, F.; Lye, G., Impact of aeration strategies on fed-batch cell culture kinetics in a single-use 24-well miniature bioreactor. *Biochemical engineering journal* **2014,** *82*, 105-116.
4. Chen, X.; Liang, Z.; Li, D.; Xiong, Y.; Xiong, P.; Guan, Y.; Hou, S.; Hu, Y.; Chen, S.; Liu, G., Microfluidic dielectrophoresis device for trapping, counting and detecting Shewanella oneidensis at the cell level. *Biosensors and Bioelectronics* **2018,** *99*, 416-423.
5. Weuster-Botz, D.; Stevens, S.; Hawrylenko, A., Parallel-operated stirred-columns for microbial process development. *Biochemical engineering journal* **2002,** *11* (1), 69-72.
6. Kaminski, T. S.; Scheler, O.; Garstecki, P., Droplet microfluidics for microbiology: techniques, applications and challenges. *Lab on a Chip* **2016,** *16* (12), 2168-2187.
7. Zhao, C. X.; Dwyer, M. D.; Yu, A. L.; Wu, Y.; Fang, S.; Middelberg, A. P., A simple and low-cost platform technology for producing pexiganan antimicrobial peptide in E. coli. *Biotechnol Bioeng* **2015,** *112* (5), 957-64. DOI: 10.1002/bit.25505.
8. Wibowo, D.; Yang, G. Z.; Middelberg, A. P.; Zhao, C. X., Non-chromatographic bioprocess engineering of a recombinant mineralizing protein for the synthesis of silica nanocapsules. *Biotechnol Bioeng* **2017,** *114* (2), 335-343. DOI: 10.1002/bit.26079.
9. Duetz, W. A.; Rüedi, L.; Hermann, R.; O'Connor, K.; Büchs, J.; Witholt, B., Methods for intense aeration, growth, storage, and replication of bacterial strains in microtiter plates. *Appl. Environ. Microbiol.* **2000,** *66* (6), 2641-2646.
10. Warringer, J.; Blomberg, A., Automated screening in environmental arrays allows analysis of quantitative phenotypic profiles in Saccharomyces cerevisiae. *Yeast* **2003,** *20* (1), 53-67.
11. Klein, A. M.; Mazutis, L.; Akartuna, I.; Tallapragada, N.; Veres, A.; Li, V.; Peshkin, L.; Weitz, D. A.; Kirschner, M. W., Droplet barcoding for single-cell transcriptomics applied to embryonic stem cells. *Cell* **2015,** *161* (5), 1187-1201.
12. Whitesides, G. M., The origins and the future of microfluidics. *Nature* **2006,** *442* (7101), 368.
13. Weibel, D. B.; DiLuzio, W. R.; Whitesides, G. M., Microfabrication meets microbiology. *Nature Reviews Microbiology* **2007,** *5* (3), 209.
14. Saleh-Lakha, S.; Trevors, J. T., Perspective: microfluidic applications in microbiology. *Journal of microbiological methods* **2010,** *82* (1), 108-111.
15. Lee, J.-H.; Kaplan, J. B.; Lee, W. Y., Microfluidic devices for studying growth and detachment of Staphylococcus epidermidis biofilms. *Biomedical microdevices* **2008,** *10* (4), 489-498.
16. Ran, R.; Sun, Q.; Baby, T.; Wibowo, D.; Middelberg, A. P. J.; Zhao, C. X., Multiphase microfluidic synthesis of micro- and nanostructures for pharmaceutical applications. *Chem Eng Sci* **2017,** *169*, 78-96. DOI: 10.1016/j.ces.2017.01.008.
17. Wang, H. F.; Ran, R.; Liu, Y.; Hui, Y.; Zeng, B. J.; Chen, D.; Weitz, D. A.; Zhao, C. X., Tumor-Vasculature-on-a-Chip for Investigating Nanoparticle Extravasation and Tumor Accumulation. *Acs Nano* **2018,** *12* (11), 11600-11609. DOI: 10.1021/acsnano.8b06846.
18. Zanzotto, A.; Szita, N.; Boccazzi, P.; Lessard, P.; Sinskey, A. J.; Jensen, K. F., Membrane-aerated microbioreactor for high-throughput bioprocessing. *Biotechnology and bioengineering* **2004,** *87* (2), 243-254.

19. Boccazzi, P.; Zhang, Z.; Kurosawa, K.; Szita, N.; Bhattacharya, S.; Jensen, K. F.; Sinskey, A. J., Differential gene expression profiles and real-time measurements of growth parameters in Saccharomyces cerevisiae grown in microliter-scale bioreactors equipped with internal stirring. *Biotechnology progress* **2006,** *22* (3), 710-717.
20. Zanzotto, A.; Boccazzi, P.; Gorret, N.; Van Dyk, T. K.; Sinskey, A. J.; Jensen, K. F., In situ measurement of bioluminescence and fluorescence in an integrated microbioreactor. *Biotechnology and bioengineering* **2006,** *93* (1), 40-47.
21. Steinhaus, B.; Garcia, M. L.; Shen, A. Q.; Angenent, L. T., A portable anaerobic microbioreactor reveals optimum growth conditions for the methanogen Methanosaeta concilii. *Appl. Environ. Microbiol.* **2007,** *73* (5), 1653-1658.
22. Edlich, A.; Magdanz, V.; Rasch, D.; Demming, S.; Aliasghar Zadeh, S.; Segura, R.; Kähler, C.; Radespiel, R.; Büttgenbach, S.; Franco-Lara, E., Microfluidic reactor for continuous cultivation of Saccharomyces cerevisiae. *Biotechnology progress* **2010,** *26* (5), 1259-1270.
23. Alam, M. N. H. Z.; Schäpper, D.; Gernaey, K. V., Embedded resistance wire as a heating element for temperature control in microbioreactors. *Journal of Micromechanics and Microengineering* **2010,** *20* (5), 055014.
24. van Leeuwen, M.; Krommenhoek, E. E.; Heijnen, J. J.; Gardeniers, H.; van der Wielen, L. A.; Van Gulik, W. M., Aerobic batch cultivation in micro bioreactor with integrated electrochemical sensor array. *Biotechnology progress* **2010,** *26* (1), 293-300.
25. Luo, X.; Shen, K.; Luo, C.; Ji, H.; Ouyang, Q.; Chen, Y., An automatic microturbidostat for bacterial culture at constant density. *Biomedical microdevices* **2010,** *12* (3), 499-503.
26. Sun, Q.; Tan, S. H.; Chen, Q. S.; Ran, R.; Hui, Y.; Chen, D.; Zhao, C. X., Microfluidic Formation of Coculture Tumor Spheroids with Stromal Cells As a Novel 3D Tumor Model for Drug Testing. *Acs Biomater Sci Eng* **2018,** *4* (12), 4425-4433. DOI: 10.1021/acsbiomaterials.8b00904.
27. Hol, F. J.; Dekker, C., Zooming in to see the bigger picture: Microfluidic and nanofabrication tools to study bacteria. *Science* **2014,** *346* (6208), 1251821.
28. Liu, Z.; Banaei, N.; Ren, K., Microfluidics for Combating Antimicrobial Resistance. *Trends in biotechnology* **2017,** *35* (12), 1129-1139.
29. Tan, S. H.; Nguyen, N.-T.; Chua, Y. C.; Kang, T. G., Oxygen plasma treatment for reducing hydrophobicity of a sealed polydimethylsiloxane microchannel. *Biomicrofluidics* **2010,** *4* (3), 032204.
30. Xi, H.-D.; Guo, W.; Leniart, M.; Chong, Z. Z.; Tan, S. H., AC electric field induced droplet deformation in a microfluidic T-junction. *Lab on a Chip* **2016,** *16* (16), 2982-2986. DOI: 10.1039/C6LC00448B.
31. Huebner, A.; Bratton, D.; Whyte, G.; Yang, M.; Demello, A. J.; Abell, C.; Hollfelder, F., Static microdroplet arrays: a microfluidic device for droplet trapping, incubation and release for enzymatic and cell-based assays. *Lab on a Chip* **2009,** *9* (5), 692-698.
32. Courtois, F.; Olguin, L. F.; Whyte, G.; Theberge, A. B.; Huck, W. T.; Hollfelder, F.; Abell, C., Controlling the retention of small molecules in emulsion microdroplets for use in cell-based assays. *Analytical chemistry* **2009,** *81* (8), 3008-3016.
33. Dewan, A.; Kim, J.; McLean, R. H.; Vanapalli, S. A.; Karim, M. N., Growth kinetics of microalgae in microfluidic static droplet arrays. *Biotechnology and Bioengineering* **2012,** *109* (12), 2987-2996. DOI: 10.1002/bit.24568.
34. Cormack, B. P.; Valdivia, R. H.; Falkow, S., FACS-optimized mutants of the green fluorescent protein (GFP). *Gene* **1996,** *173* (1), 33-38.

35. Bridle, H., Chapter Five - Optical Detection Technologies for Waterborne Pathogens. In *Waterborne Pathogens*, Bridle, H., Ed. Academic Press: Amsterdam, 2014; pp 119-145. DOI: https://doi.org/10.1016/B978-0-444-59543-0.00005-0.
36. Giladi, M.; Porat, Y.; Blatt, A.; Wasserman, Y.; Kirson, E. D.; Dekel, E.; Palti, Y., Microbial growth inhibition by alternating electric fields. *Antimicrobial agents and chemotherapy* **2008,** *52* (10), 3517-3522.
37. Giladi, M.; Porat, Y.; Blatt, A.; Shmueli, E.; Wasserman, Y.; Kirson, E. D.; Palti, Y., Microbial growth inhibition by alternating electric fields in mice with Pseudomonas aeruginosa lung infection. *Antimicrobial agents and chemotherapy* **2010,** *54* (8), 3212-3218.
38. Nakanishi, K.; Tokuda, H.; Soga, T.; Yoshinaga, T.; Takeda, M., Effect of electric current on growth and alcohol production by yeast cells. *Journal of Fermentation and Bioengineering* **1998,** *85* (2), 250-253.
39. Liao, D. S.; Raveendran, J.; Golchi, S.; Docoslis, A., Fast and sensitive detection of bacteria from a water droplet by means of electric field effects and micro-Raman spectroscopy. *Sensing and Bio-Sensing Research* **2015,** *6*, 59-66. DOI: https://doi.org/10.1016/j.sbsr.2015.09.005.
40. Chen, X.; Liang, Z.; Li, D.; Xiong, Y.; Xiong, P.; Guan, Y.; Hou, S.; Hu, Y.; Chen, S.; Liu, G.; Tian, Y., Microfluidic dielectrophoresis device for trapping, counting and detecting Shewanella oneidensis at the cell level. *Biosensors and Bioelectronics* **2018,** *99*, 416-423. DOI: https://doi.org/10.1016/j.bios.2017.08.017.
41. Lagally, E. T.; Lee, S.-H.; Soh, H., Integrated microsystem for dielectrophoretic cell concentration and genetic detection. *Lab on a Chip* **2005,** *5* (10), 1053-1058.
42. Juergensmeyer, M. A.; Nelson, E. S.; Juergensmeyer, E. A., Shaking alone, without concurrent aeration, affects the growth characteristics of Escherichia coli. *Letters in Applied Microbiology* **2007,** *45* (2), 179-183. DOI: 10.1111/j.1472-765X.2007.02172.x.
43. Sezonov, G.; Joseleau-Petit, D.; D'Ari, R., Escherichia coli Physiology in Luria-Bertani Broth. *Journal of Bacteriology* **2007,** *189* (23), 8746-8749. DOI: 10.1128/jb.01368-07.
44. Boedicker, J. Q.; Vincent, M. E.; Ismagilov, R. F., Microfluidic Confinement of Single Cells of Bacteria in Small Volumes Initiates High-Density Behavior of Quorum Sensing and Growth and Reveals Its Variability. *Angewandte Chemie International Edition* **2009,** *48* (32), 5908-5911. DOI: 10.1002/anie.200901550.
45. Boedicker, J. Q.; Li, L.; Kline, T. R.; Ismagilov, R. F., Detecting bacteria and determining their susceptibility to antibiotics by stochastic confinement in nanoliter droplets using plug-based microfluidics. *Lab on a Chip* **2008,** *8* (8), 1265-1272.